Space Sci Rev (2012) 172:271–282
DOI 10.1007/s11214-011-9766-z

Emerging Parameter Space Map of Magnetic Reconnection in Collisional and Kinetic Regimes

William Daughton · Vadim Roytershteyn

Received: 5 August 2010 / Accepted: 28 February 2011 / Published online: 25 March 2011

Abstract In large-scale systems of interest to solar physics, there is growing evidence that magnetic reconnection involves the formation of extended current sheets which are unstable to plasmoids (secondary magnetic islands). Recent results suggest that plasmoids may play a critical role in the evolution of reconnection, and have raised fundamental questions regarding the applicability of resistive MHD to various regimes. In collisional plasmas, where the thickness of all resistive layers remain larger than the ion gyroradius, simulations results indicate that plasmoids permit reconnection to proceed much faster than the slow Sweet-Parker scaling. However, it appears these rates are still a factor of $\sim 10\times$ slower than observed in kinetic regimes, where the diffusion region current sheet falls below the ion gyroradius and additional physics beyond MHD becomes crucially important. Over a broad range of interesting parameters, the formation of plasmoids may naturally induce a transition into these kinetic regimes. New insights into this scenario have emerged in recent years based on a combination of linear theory, fluid simulations and fully kinetic simulations which retain a Fokker-Planck collision operator to allow a rigorous treatment of Coulomb collisions as the reconnection electric field exceeds the runaway limit. Here, we present some new results from this approach for guide field reconnection. Based upon these results, a parameter space map is constructed that summarizes the present understanding of how reconnection proceeds in various regimes.

Keywords Magnetic · Reconnection · Plasmoids

1 Introduction

Magnetic reconnection is important in a diverse range of plasma phenomena including planetary magnetospheres, magnetic fusion machines and a wide variety of astrophysical

W. Daughton (✉) · V. Roytershteyn
Los Alamos National Laboratory, MS F699, Los Alamos, NM, USA
e-mail: daughton@lanl.gov

V. Roytershteyn
e-mail: roytersh@lanl.gov

settings. In solar physics, observations suggest that magnetic reconnection occurs in the corona, chromosphere, and transition region, making it a truly ubiquitous and important phenomenon for understanding the atmosphere of our Sun. Abundant evidence of solar reconnection has been obtained in the last two decades [see for example reviews in Shibata (1999), Martens (2003) and more recently Isobe and Shibata (2009)]. Pioneering Yohkoh observations put on firm ground long-conjectured association of solar flares with reconnection. Examples of important discoveries include observations of cusp-shaped post-flare loops (Tsuneta et al. 1992), of hard X-ray sources located in the magnetic cusp region above the soft-X ray loops in impulsive flares (Masuda et al. 1994), and of plasmoid ejections in impulsive flares (Shibata et al. 1995). SOHO, TRACE and RHESSI have produced further evidence, notably the characterization of reconnection inflows (Yokoyama et al. 2001; Chen et al. 2004; Lin et al. 2005). Observations of solar flares suggest a highly intermittent in space and time character of reconnection, as was inferred for example from TRACE observations of fine structures in flare ribbons (Fletcher et al. 2004) and observations of drifting pulsating structures (Karlicky et al. 2005). The radio pulsations exhibit power-law spectra and are thought to be a manifestation of electron beams accelerated in multi-scale reconnection process reminiscent of Shibata and Tanuma (2001). Reconnection is also believed to be active in the lower solar atmosphere, where the plasma is partially ionized and the resistivity is significantly higher. Chromospheric jets (Innes et al. 1997; Shibata et al. 2007), canceling magnetic features in the lower solar atmosphere (Litvinenko and Martin 1999), and frequent, short-lived H_α brightenings known as Ellerman bombs (Georgoulis et al. 2002) are all thought to be associated with magnetic reconnection.

Despite this growing body of observational evidence, there remain some major challenges in understanding how magnetic reconnection actually proceeds in these large-scale systems for the widely different parameter regimes that occur in the chromosphere, transition region and corona. Very broadly, the difficulties lie in bridging the gap between the dynamics at macroscopic scales and the microphysics of reconnection. Efforts to understand fast reconnection in large systems have been historically motivated by the dramatic inadequacy of the Sweet-Parker model (Parker 1957), which predicts that the reconnection rate scales as $R = U_{in}/V_A \approx \delta_{sp}/L_{sp} \approx S^{-1/2}$ where U_{in} is the inflow velocity, $V_A = B_o/\sqrt{4\pi m_i n}$ is Alfvén velocity, B_o is the reconnecting component of the magnetic field upstream of the layer, n is the plasma density, δ_{sp} is the half-thickness and L_{sp} is the half-length of the layer, $S = 4\pi V_A L_{sp}/\eta c^2$ is the Lundquist number and η is the resistivity. Assuming classical resistivity due to Coulomb collisions yields $R \sim 10^{-6}$ for typical coronal parameters, vastly smaller than $R = 0.001 \rightarrow 0.1$ inferred from observations of flares (see e.g. Narukage and Shibata 2006 and references therein).

In order to explain these observations, proposed models of fast reconnection must produce rates that are nearly independent of the system size and dissipation mechanism. The slow scaling in the Sweet-Parker (SP) model arises from the highly elongated current sheets at large S, and researchers have sought to circumvent this problem by a variety of mechanisms. The Petschek model offers one possible solution (Petschek 1964), but extensive MHD simulations have demonstrated that the Petschek-type solutions require localized dissipation coefficients, while uniform resistivity leads to elongated SP layers (Ugai and Tsuda 1977; Biskamp 1986; Yan et al. 1992; Uzdensky and Kulsrud 2000). However, as researchers were able to push these simulations to higher Lundquist numbers $S \gtrsim S_{crit} \sim 10^4$, it became clear that the elongated SP layers are unstable to secondary magnetic islands (or plasmoids) (Matthaeus and Lamkin 1985; Biskamp 1986; Fu and Lee 1986; Yan et al. 1992; Malara et al. 1992). These numerical results along with observations of plasmoid ejection and the inferred intermittent nature of reconnection in the corona motivated researchers to propose that plasmoids may play a key role in mediating fast reconnection (Kliem et al. 2000; Shibata and Tanuma 2001). In recent years, the foundation for these ideas has been greatly strengthened by analytic theory for the plasmoid instability (Loureiro et al. 2007; Ni et al. 2010) which has been carefully verified with MHD simulations (Samtaney et al. 2009; Bhattacharjee et al. 2009; Huang and Bhattacharjee 2010). Within the linear regime, these results predict a growth rate that scales as $S^{1/4}V_A/L_{sp}$ with the number of plasmoids increasing with $S^{3/8}$. Thus the instability is increasingly violent in high-S regimes, and simulations demonstrate that plasmoids grow to large amplitude and breakup the layer before they are convected downstream by the Alfvénic outflow. As this occurs, new current sheets form between islands which can also be unstable to plasmoids. This leads to many more plasmoids than predicted by the linear theory and gives rise to average macroscopic reconnection rates $R \sim 0.01$ that are weakly dependent on resistive dissipation (Lapenta 2008; Bhattacharjee et al. 2009; Huang and Bhattacharjee 2010).

These new results suggests that magnetic reconnection in solar applications may proceed through a hierarchy of current sheets and islands as originally proposed by Shibata and Tanuma (2001). For many solar applications, this may lead to the breakdown of the MHD model when new current sheets between islands approach the ion kinetic scale. For Lundquist numbers below the critical value for plasmoids $S < S_{crit}$, two-fluid theory and simulations predict a transition to faster reconnection in neutral sheet geometry when $\delta_{sp} < d_i$ where d_i is an ion inertial length (Ma and Bhattacharjee 1996; Cassak et al. 2005; Simakov and Chacón 2008). With a guide field, the transition away from MHD is predicted to occur when $\delta_{sp} \leq \rho_s$ (where ρ_s is an ion gyroradius based on the acoustic speed). Laboratory reconnection experiments have confirmed these basic transition conditions for both the neutral sheet limit (Yamada et al. 2006) and for strong guide fields (Egedal et al. 2006).

In these *kinetic* regimes, a variety of two-fluid and kinetic models predict reconnection rates that are weakly dependent on the system size or dissipation mechanism (Birn et al. 2001; Hesse et al. 2001; Pritchett 2001; Shay et al. 2001). Unfortunately, there remain uncertainties in the precise scalings for both fluid models (Bhattacharjee et al. 2005) and fully kinetic particle-in-cell (PIC) simulations which feature profound differences (Daughton et al. 2006) in the structure of the electron layers in comparisons to reduced fluid models. In particular, the PIC simulations feature highly elongated electron layers with a complicated two-scale structure (Daughton et al. 2006; Karimabadi et al. 2007; Shay et al. 2007). These layers are generally unstable to plasmoid formation leading to a time-dependent reconnection process in which electron physics may play important role (Daughton et al. 2006; Karimabadi et al. 2007; Klimas et al. 2008; Wan and Lapenta 2008; Daughton et al. 2011b). Despite these ongoing uncertainties, it is important to emphasize that the properly normalized reconnection rates in all of these kinetic studies $R \approx 0.04 \rightarrow 0.2$ is still quite fast, and there are good reasons to believe this will hold for larger systems.

In order to better understand the transition between fluid and kinetic regimes, we have recently employed fully kinetic PIC simulations with a Monte-Carlo treatment of the Fokker-Planck collision operator (Daughton et al. 2009a). Although the required numerical methods (Takizuka and Abe 1977) were developed decades ago, sufficient computing power to employ this approach for reconnection studies became available only recently (Bowers et al. 2008, 2009). This approach permits a direct solution of the full plasma kinetic equation, which forms the theoretical basis for all fluid models. This allows a rigorous treatment of the reconnection dynamics and dissipation mechanism as the reconnection electric field exceeds the runaway limit (Roytershteyn et al. 2010). For relatively low Lundquist numbers $S \sim 10^3$, this new approach recovers the Sweet-Parker scaling and the transition to the faster kinetic regime near the predicted threshold $\delta_{sp} < d_i$ (Daughton et al. 2009a). However, for higher S the extended SP layers are unstable to plasmoid formation leading to a breakup of the layer and the formation of new current layers between the islands (Daughton et al. 2009b). When the thickness of these layers approach d_i, a significant enhancement in the reconnection rate is observed as the dynamics transition into the kinetic regime.

These new results suggest that in large systems plasmoids may naturally push the evolution towards small scales where kinetic effects become essential in the reconnection process. In this work, we extend these previous results to consider this same scenario in guide field regimes, which are far more relevant for the solar applications. These collisional kinetic simulations confirm the basic hypothesis regarding the role of plasmoids. Using simple scaling arguments, we demonstrate that plasmoids may lead to a natural transition to kinetic scales over a broad range of parameter regimes of relevance to solar applications. These results are conveniently summarized in a parameter space map, which allows researchers to quickly estimate how reconnection will proceed. Many of the ideas discussed in this manuscript naturally complement the review given by Cassak and Shay (2011) in this volume.

2 Time Scales and Simple Transition Estimates

Here, we quickly review the transition criteria assuming the SP layer is structurally stable (no plasmoids). The upstream reconnecting component of the magnetic field is denoted by B_o, the total magnetic field is B_T and the central layer density is n_o. The predicted two-fluid transition criteria (Cassak et al. 2005; Uzdensky 2007) is $\delta_{sp} \lesssim d_i$ for weak guide fields or $\delta_{sp} \lesssim \rho_s$ for strong guide fields, where $d_i = c/\omega_{pi}$ with $\omega_{pi} = \sqrt{(4\pi n_o e^2)/m_i}$ and ρ_s is the ion-sound radius (i.e. based on the electron temperature, the ion mass, and the total magnetic field). Even within simulations, there are some order unity uncertainties when applying these estimates. In real plasmas, there are a much wider range of uncertainties to consider, along with some physical constraints that allow both strong and weak field limits to be considered together.

Within the collisional SP regime, the ion and electron temperatures are closely coupled, since the transit time for plasma through the diffusion region $\tau_A = L_{sp}/V_A$ is long in comparison to the collisional time scale τ_{eq} for thermal equilibration

$$\frac{\tau_A}{\tau_{eq}} \sim \left(\frac{\delta_{sp}}{d_i}\right)^2 . \tag{1}$$

Thus when considering the initial transition away from collisional reconnection, it is appropriate to assume $T_e \approx T_i$, which implies $\rho_s \approx \rho_i$ where $\rho_i = v_{th_i}/\Omega_{ci}$ is thermal ion gyoradius, $v_{th_i} = (2T_i/m_i)^{1/2}$ is the ion thermal velocity and $\Omega_{ci} = eB_T/(m_i c)$ is the ion cyclotron frequency. Note that $\rho_i \approx d_i(\beta/2)^{1/2}$ where $\beta = 8\pi n_o(T_i + T_e)/B_T^2$, and for weak guide field $B_T \approx B_o$ the force balance across the layer requires $\beta = 1 + \beta_{up}$ where β_{up} is based on the local conditions immediately upstream of the layer. For most applications of interests $\beta_{up} \lesssim 1$ and thus $\rho_i \sim d_i$ for weak guide fields. Neglecting these order unity factors, we can conveniently express the approximate transition criteria for arbitrary guide field as

$$\begin{aligned} \delta_{sp} &\gtrsim \rho_i \quad \rightarrow \text{Collisional Regime}, \\ \delta_{sp} &\lesssim \rho_i \quad \rightarrow \text{Kinetic Regime}. \end{aligned} \tag{2}$$

To apply this criteria, we remind readers that ρ_i is based on the total magnetic field B_T, while V_A, S and δ_{sp} should be computed using the reconnecting component of the magnetic field B_o. While in simulations both B_o and B_T are precisely known, in solar applications these are very hard to distinguish. Together with uncertainties in density, temperature and macroscopic scales, (2) can only be estimated to within an order-of-magnitude at best for solar applications. To simplify the discussion in this manuscript, we assume that the force balance across the SP layers is always determined through the pressure term which implies that $B_o/B_T \approx \beta^{1/2}$.

In order to make scaling predictions, it is useful to re-write this transition criteria in terms of a critical resistivity. Sweet-Parker theory does not really predict the length of the diffusion region current sheet, but only the aspect ratio. However, simulations clearly indicate that the length of the SP layer L_{sp} scales with the global system size L before the onset of plasmoids. We denote the dimensionless resistivity as

$$\hat{\eta} \equiv \frac{\nu_{ei}}{\Omega_{ce}} \frac{B_T}{B_o},$$

where ν_{ei} is the electron-ion collision frequency and $\Omega_{ce} = eB_T/(m_e c)$ is the electron cyclotron frequency. In this system of units, the Lundquist number is $S = L_{sp}/(d_i \hat{\eta})$. In simulations with periodic boundary conditions, $L_{sp} \approx L/4$ is a reasonable estimate but in large open systems this may be somewhat different. With an estimate for the layer length, it is straight forward to determine the critical resistivity that corresponds to $\delta_{sp} < \rho_i$

$$\hat{\eta}_c \lesssim \beta \frac{d_i}{L_{sp}} \approx 4\beta \left(\frac{d_i}{L}\right). \tag{3}$$

Thus for Lundquist numbers larger than $S > L_{sp}/(d_i \hat{\eta}_c)$, the reconnection dynamics will always be in a kinetic regime.

When considering these types of estimates, it is important to remember that collisional resistivity is only valid when the reconnection electric field E_r is significantly below the Dreicer runaway limit $E_D \equiv (m_e T_e)^{1/2} \nu_{ei}/e$. Using the Sweet-Parker scaling, this ratio can be expressed as

$$\frac{E_r}{E_D} \sim \left(\frac{m_e}{m_i}\right)^{1/2} \frac{\rho_i}{\delta_{sp}} \beta^{-1/2},$$

which implies that for $\beta > m_e/m_i$ the resistive layers will first encounter the ρ_i scale before runaway fields are produced. Collisional regimes $\delta_{sp} > \rho_i$ are expected to be sub-Dreicer, unless the guide field is extremely strong such that $\beta < m_e/m_i$. In this limit, it is possible to produce runaway fields before encountering kinetic scales, and the transition physics may be quite different. However, for the range of β of most interest in solar applications, it appears this is not the case and (2)–(3) are the relevant comparisons.

When reconnection is faster than Sweet-Parker, it is quite easy to create runaway fields. Indeed, simple estimates for the solar corona imply that the reconnection electric field is typically orders of magnitude larger than the Dreicer limit. For a given reconnection rate R, this ratio is approximately

$$\frac{E_r}{E_D} \sim \frac{R}{\hat{\eta}} \left(\frac{m_e}{m_i}\right)^{1/2}, \tag{4}$$

The runaway limit $E_r \sim E_D$ then corresponds to a Lundquist number of

$$S_D \sim \frac{\sqrt{\beta}}{R} \left(\frac{m_i}{m_e}\right)^{1/2} \left(\frac{L_{sp}}{\rho_i}\right), \tag{5}$$

which allows us to quickly identify the onset of runaway regimes for the parameter space map discussed in Sect. 5.

3 Influence of Plasmoids on Transition

The formation of plasmoids within a Sweet-Parker layer has profound implications for both the reconnection rate and the transition to kinetic regimes. Here we summarize the basic thinking on these issues from recent papers (Daughton et al. 2009b; Cassak and Drake 2009; Cassak et al. 2009; Huang and Bhattacharjee 2010; Uzdensky et al. 2010). As illustrated in Fig. 1, we assume that N_p plasmoids form within the original SP layer and that the new layers between the islands also follow the same SP scaling but with a reduced layer length $\sim L_{sp}/N_p$. This implies the thickness δ of the new layers scales as $\delta/\delta_{sp} \sim 1/\sqrt{N_p}$ where δ_{sp} is the half-thickness of the original SP layer. When $N_p \gg 1$, it is possible to reach kinetic scales $\delta \leq \rho_i$ much sooner than (3) where it was assumed that the SP layer was structurally stable with a length L_{sp} that scales with the global system size L.

If the new current layers remain thicker than the ion gyroscale $\delta > \rho_i$, the influence of plasmoids should be well described by MHD. In the past year, researchers have confirmed that new layers also appear to follow the SP scaling relationships (Cassak et al. 2009), but with reduced layer lengths due to the plasmoids. Assuming the number of plasmoids N_p scales as

$$N_p \sim \left(\frac{S}{S_{crit}}\right)^{\alpha}, \tag{6}$$

when the Lundquist number is larger than the critical value for the onset of plasmoids $S_{crit} \sim 10^4$, one can easily show that the reconnection rate for $S > S_{crit}$ is approximately

$$R \equiv \frac{cE_r}{B_o V_A} \approx S^{(\alpha-1)/2} S_{crit}^{-\alpha/2}. \tag{7}$$

Likewise, the critical resistivity which will produce resistive layers approaching kinetic scales $\delta \approx \rho_i$ can be written as

$$\hat{\eta}_c \sim \frac{\beta^{1/(1+\alpha)}}{S_{crit}^{\alpha/(1+\alpha)}} \left(\frac{d_i}{L_{sp}}\right)^{\frac{1-\alpha}{1+\alpha}}. \tag{8}$$

For example, using the analytic prediction $\alpha = 3/8$ from Loureiro et al. (2007), would imply a scaling for the reconnection rate $R \sim S^{-5/16}$. While this is faster than the classic SP scaling $S^{-1/2}$ it would still be very slow for most solar applications. However, the linear theory breaks down very quickly and all simulations report many more islands with scaling

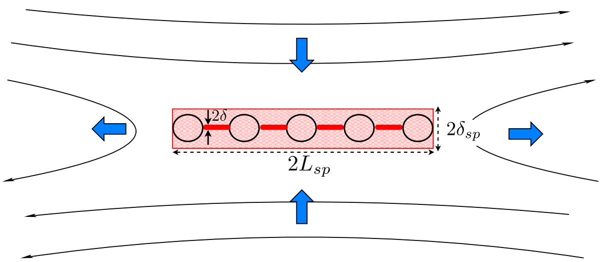

Fig. 1 Geometry of a Sweet-Parker layer that is unstable to plasmoids

coefficients in the range $\alpha \approx 0.6 \to 1$ (Daughton et al. 2009b; Bhattacharjee et al. 2009; Cassak and Drake 2009; Huang and Bhattacharjee 2010). In fact, the only way to verify the linear theory is to design the simulation studies to examine just the initial breakup (Samtaney et al. 2009). Beyond this point, the new current sheets between the plasmoids can also be unstable to new plasmoids.

To roughly account for these effects, we can sketch out estimates for the high-S regime in two different ways. First, one may directly count the numbers of plasmoids within the MHD simulations as a function of S and examine the functional dependence. The most careful studies to date (Huang and Bhattacharjee 2010) indicate that $N_p \sim S$ in the limit where $S \gg S_{crit}$. Taking $\alpha \to 1$ in (7) implies a reconnection rate of $R \approx S_{crit}^{-1/2} \sim 0.01$ that is independent of the resistive dissipation. Another way to look at the problem is to assume some scaling coefficient $\alpha < 1$ is valid for each new current sheet within the hierarchy. If the basic scenario in Fig. 1 is applied recursively until the Lundquist number of the new current sheets fall below S_{crit}, then the precise value of α no longer matters for $S \gg S_{crit}$. The reconnection rate is again set by the limiting value $R \approx S_{crit}^{-1/2}$. It is comforting that both ways of looking at the problem give the same result in the limit of $S \gg S_{crit}$.

These new results represent a profound change in thinking from just a few years ago. In the parameter regime relevant to the solar corona $S \sim 10^{12}$, this new estimate the for collisional reconnection rate is a factor of 10^4 faster than the classic Sweet-Parker scaling. However, there are two important issues to keep in mind. First, these MHD simulations are only 2D and are still limited to $S < 10^7$; so it is possible that new surprises may still emerge. Second, if these results hold up as we have outlined above, it implies that the MHD model will break down over a broad range of interesting parameters, due to the unavoidable transition to kinetic scales. For example, taking the limit $\alpha \to 1$ in (8)

$$\hat{\eta}_c = \frac{\nu_{ei}}{\Omega_{ce}} \frac{B_T}{B_o} \sim \frac{\beta^{1/2}}{S_{crit}^{1/2}}, \tag{9}$$

implies that reconnection will always hit kinetic scales in large-scale plasmas, whenever the electron-ion collision frequency falls below $\nu_{ei} \lesssim 0.01\Omega_{ce}\beta$. Since the reconnection rate is roughly $\sim 10\times$ larger in the kinetic regime, this implies that most of the energy release will still occur through kinetic mechanisms (Shepherd and Cassak 2010).

4 Collisional Kinetic Simulations with a Guide Field

Including a Fokker-Planck collision operator within a fully kinetic simulation is a powerful approach to study the influence of plasmoid formation on the transition to kinetic regimes, and the transition between sub-Dreicer and super-Dreicer fields (Roytershteyn et al. 2010). Recent studies examining the influence of plasmoids focused on the limit of a neutral sheet (Daughton et al. 2009a, 2009b), while the guide field limit is more appropriate for solar applications. Here we consider some preliminary results from a guide field simulation that support the basic scenario described in the previous section.

The simulations were performed with the VPIC code (Bowers et al. 2008) which has been modified to include Coulomb collisions and benchmarked against transport theory (Daughton et al. 2009a). The initial condition is a Harris sheet with magnetic field $B_x = B_o \tanh(z/\lambda)$ and density $n = n_o \mathrm{sech}^2(z/\lambda)$ provided by drifting Maxwellian distributions with uniform temperature $T_e = T_i = T_o$ ($\lambda = 2d_i$ is the half-thickness of the current sheet). A uniform non-drifting background is included with density $n_b = 0.3n_o$ and equal temperature. The guide field for this example is $B_y = B_o$. Other parameters are $m_i/m_e = 40$, $\omega_{pe}/\Omega_{ce} = \sqrt{2}$, where $\omega_{pe} = \sqrt{(4\pi n_o e^2)/m_e}$ is the electron plasma frequency, $v_{the}/c = 0.35$ where $v_{the} = (2T_o/m_e)^{1/2}$ is the electron thermal speed. Lengths are normalized to the ion inertial scale $d_i = c/\omega_{pi}$ where $\omega_{pi} = \sqrt{(4\pi n_o e^2)/m_i}$ and time is normalized to $\Omega_{ci} = eB_T/(m_i c)$ (where $B_T = (B_y^2 + B_o^2)^{1/2} = (2)^{1/2} B_o$). The time step is $\Delta t \omega_{pe} = 0.065$ and the boundary conditions are periodic in the x-direction while the z-boundaries are conducting for fields and reflecting for particles. The 2D domain size is $400 d_i \times 100 d_i$, with 6400×1600 cells and 1000 particles per cell.

With a Fokker-Planck treatment of Coulomb collisions, the dimensionless perpendicular $\hat{\eta}_\perp$ and parallel $\hat{\eta}_{||}$ resistivities vary in both space and time due to Ohmic heating within the layer

$$\begin{aligned} \hat{\eta}_\perp &\equiv \frac{\omega_{pi}^2}{4\pi\Omega_{ci}} \frac{B_T}{B_o} \eta_\perp = \hat{\eta}_{\perp o} \left(\frac{T_o}{T_e} \right)^{3/2}, \\ \hat{\eta}_{||} &= 0.51 \hat{\eta}_\perp, \end{aligned} \tag{10}$$

where $\eta_\perp \equiv m_e \nu_{ei}/(e^2 n_e)$ is the resistivity perpendicular to the magnetic field, T_e the local electron temperature and $\hat{\eta}_{\perp o} = 0.04$ is the initial dimensionless resistivity for this study. For guide field reconnection, the parallel resistivity $\hat{\eta}_{||}$ is most relevant for setting the structure of the SP layer. The initial resistivity is a factor of $\sim 4\times$ larger than the transition estimate in (2) which implies that Ohmic heating alone cannot give rise to a transition, since the temperature is eventually limited by the pressure balance requirement across the layer (Daughton et al. 2009a).

The evolution of the current density for this case is given in Fig. 2. During the initial phase $t\Omega_{ci} = 0 \rightarrow 90$, a well developed Sweet-Parker layer is formed as illustrated in the

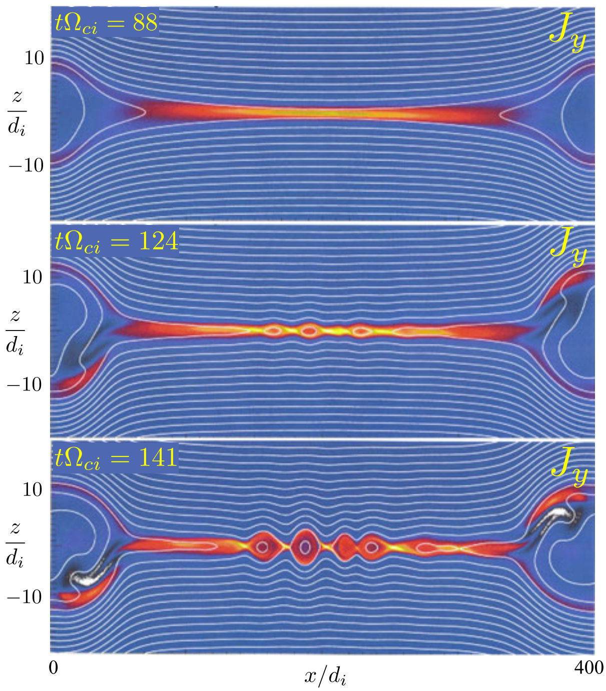

Fig. 2 Evolution of the current density J_y for a collisional kinetic simulation with a guide field equal to the reconnecting field. At early time $t\Omega_{ci} = 88$ in the *top panel*, a Sweet-Parker layer has formed, but as the simulation proceeds the layer becomes unstable to plasmoids which induce a transition to the kinetic regime. *White lines* are the magnetic flux surfaces and simulation parameters are given in the text

top panel. As the simulation proceeds, plasmoids are observed to grow within the resistive layer which gives rise to an enhancement in the current density between islands. An abrupt increase in the reconnection rate is observed when the thickness of these layers approach $\delta \approx \rho_i$ consistent with the expectations outlined in the previous section. However, we should emphasis that ρ_i is only a factor of 2 smaller than d_i for these parameters, so in the future it is important to consider stronger guide fields to better separate these scales. Nevertheless, these preliminary results confirm that plasmoids are playing a crucial role in facilitating the transition to kinetic regimes.

5 Summary of Results

In order to quickly understand the relevance of these results for any given problem, it is useful to summarize these scalings in graphical form using two dimensionless parameters: the global Lundquist number S and the system size in units of the ion gyroradius L/ρ_i. As illustrated in Fig. 3, this allows us to quickly summarize all of the results in this manuscript. The dashed blue line corresponds to (2) which gives the transition estimate when Sweet-Parker layers are stable ($S < S_{crit}$). For $S \gtrsim S_{crit}$ the layers are unstable and MHD calculations indicate the critical Lundquist number is $S_{crit} \sim 10^4$ as shown by the green line, but with turbulent fluctuations in the initial conditions (Matthaeus and Lamkin 1985) it appears this may be reduced to $S_{crit} \sim 2000$. This value is closer to what is observed in the collisional kinetic PIC simulations (Daughton et al. 2009a) which also have finite fluctuations from thermal noise. Regardless of the precise value, the range of parameter space where the Sweet-Parker scaling applies is really quite limited.

The solid blue line in Fig. 3 corresponds to (9). For the white region below this curve, the MHD description remains valid and reconnection will proceed through a dynamic scenario with continuous plasmoid formation. Above this curve in the yellow region, the development of plasmoids will always induce a transition to kinetic scales $\delta \le \rho_i$ and thus the MHD model is no longer valid. It is possible that two-fluid models may be valid in a limited portion of this yellow region. The two-fluid closures are most appropriate in the region where the reconnection electric field remains less than the runway limit, corresponding to the yellow region between the red and solid blue curves. From (5), one can see that the size of this

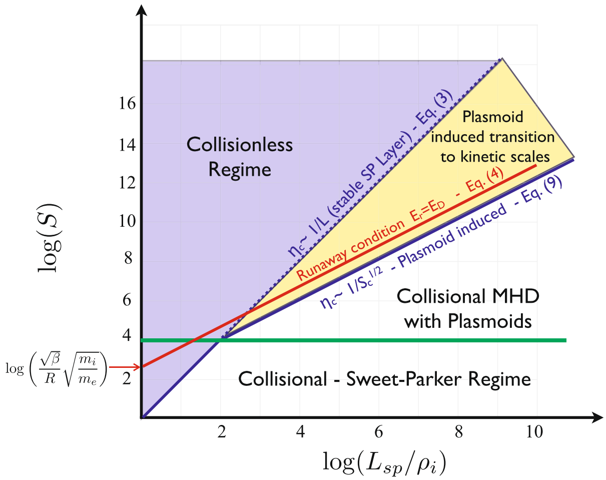

Fig. 3 Emerging parameter space map of magnetic reconnection. The *red curve* corresponds to $E_r = E_D$ and for this figure was estimated assuming a hydrogen plasma with $\beta = 0.2$ and $R = 0.05$. Note that L_{sp} is assumed to scale with macroscopic system size L

region depends on the mass ratio m_i/m_e, the plasma β and the reconnection rate. For the red curve shown in Fig. 3, we are assuming a hydrogen plasma with $\beta = 0.2$ and $R = 0.05$. For other parameters, one can quickly shift the y-intercept of this line as indicated, while keeping the slope the same.

For the yellow region in Fig. 3, the reconnection dynamics will naturally cascade to involve kinetic scales. This region is highly relevant for solar applications, including the corona, transition region and perhaps even the chromosphere, depending on parameters used in the estimates (Litvinenko and Martin 1999). However, the chromosphere has a large neutral population which bring in many complications beyond the scope of the present manuscript. Nevertheless, these results should challenge researchers to reconsider which regimes are really *collisional* and can be fully described by MHD, and which regimes are inherently kinetic.

There are at least two major uncertainties in this map. Even within the context of 2D simulations, the region of the parameter space accessible to computer simulations is fairly limited, and thus we are forced to extrapolate far beyond current state-of-the-art MHD simulations ($S \sim 10^6$) or kinetic simulations $L/\rho_i \sim 500$. At the present time, simulations studies are typically initialized with a laminar current sheet so the influence of pre-existing turbulent fluctuations remains poorly understood. As previously mentioned, it is possible that fluctuations convected into the layer may seed additional plasmoids and lower the critical Lundquist number. Finally, very little is known regarding how reconnection will actually proceed in the presence of realistic 3D dynamics. In particular, both primary and secondary magnetic islands correspond to extended flux ropes in 3D, which may interact in a variety of complex ways not possible in 2D simulation models (Daughton et al. 2011a). In addition, a wide range of other plasma instabilities may be present in 3D which may potentially influence the reconnection dynamics.

Acknowledgements We gratefully acknowledge support from the U.S. Department of Energy through the LANL/LDRD Program and from the Institutional Computing Program at Los Alamos.

References

A. Bhattacharjee, K. Germaschewski, C. Ng, Current singularities:drivers of impulsive reconnection. Phys. Plasmas **12**, 042305 (2005)

A. Bhattacharjee, Y.M. Huang, H. Yang, B. Rogers, Fast reconnection in high-Lundquist-number plasmas due to secondary tearing instabilities. Phys. Plasmas **16**, 112102 (2009)

J. Birn, J. Drake, M. Shay, B. Rogers, R. Denton, M. Hesse, M. Kuznetsova, Z. Ma, A. Bhattacharjee, A. Otto, P. Pritchett, Geospace environmental modeling (GEM) magnetic reconnection challenge. J. Geophys. Res. **106**, 3715 (2001)

D. Biskamp, Magnetic reconnection via current sheets. Phys. Fluids **29**, 1520 (1986)

K.J. Bowers, B.J. Albright, L. Yin, B. Bergen, T.J.T. Kwan, Ultrahigh performance three-dimensional electromagnetic relativistic kinetic plasma simulation. Phys. Plasmas **15**, 055703 (2008)

K. Bowers, B. Albright, L. Yin, W. Daughton, V. Roytershteyn, B. Bergen, T. Kwan, Advances in petascale kinetic simulations with VPIC and Roadrunner. J. Phys. Conf. Ser. **180**, 012055 (2009)

P.A. Cassak, J.F. Drake, The impact of microscopic magnetic reconnection on pre-flare energy storage. Astrophys. J. **707**, 158 (2009)

P.A. Cassak, M. Shay, Magnetic reconnection for coronal conditions: Reconnection rates, secondary islands and onset. Space Sci. Rev. (2011). doi:10.1007/s11214-011-9755-2

P.A. Cassak, M.A. Shay, J.F. Drake, Scaling of sweet–parker reconnection with secondary islands. Phys. Plasmas **16**, 120702 (2009)

P. Cassak, M. Shay, J. Drake, Catastrophe model for fast magnetic reconnection onset. Phys. Rev. Lett. **95**, 235002 (2005)

P. Chen, K. Shibata, D. Brooks, H. Isobe, A re-examination of the evidence for reconnection inflow. Astrophys. J. **602**, 61–64 (2004)

W. Daughton, J. Scudder, H. Karimabadi, Fully kinetic simulations of undriven magnetic reconnection with open boundary conditions. Phys. Plasmas **13**, 072101 (2006)
W. Daughton, V. Roytershteyn, B.J. Albright, H. Karimabadi, L. Yin, K.J. Bowers, Influence of coulomb collisions on the structure of reconnection layers. Phys. Plasmas **16**, 072117 (2009a)
W. Daughton, V. Roytershteyn, B.J. Albright, H. Karimabadi, L. Yin, K.J. Bowers, Transition from collisional to kinetic regimes in large-scale reconnection layers. Phys. Rev. Lett. **103**, 065004 (2009b)
W. Daughton, V. Roytershteyn, H. Karimabadi, L. Yin, B. Albright, B. Bergen, K. Bowers, Role of electron physics in the development of turbulent magnetic reconnection in collisionless plasmas. Nature Physics, (2011a, submitted)
W. Daughton, V. Roytershteyn, H. Karimabadi, L. Yin, B.J. Albright, S. Gary, K.J. Bowers, Secondary island formation in collisional and collisionless kinetic simulations of magnetic reconnection, in *AIP Conference on Modern Challenges in Nonlinear Plasma Physics*, vol. 1320, ed. by D. Vassiliadis (American Institute of Physics, College Park, 2011b), p. 144. doi:10.1063/1.3544319
J. Egedal, W. Fox, N. Katz, M. Porkolab, K. Reim, E. Zhang, Laboratory observations of spontaneous magnetic reconnection. Phys. Rev. Lett. **98**, 015003 (2006)
L. Fletcher, J. Pollock, H. Potts, Tracking of trace ultraviolet flare footpoints. Sol. Phys. **222**, 279–298 (2004)
Z. Fu, L. Lee, Multiple x line reconnection. II. the dynamics. J. Geophys. Res. **91**(A12), 13373–13383 (1986)
M. Georgoulis, D. Rust, P. Bernasconi, B. Schmieder, Statistics, morphology, and energetics of Ellerman bombs. Astrophys. J. **575**, 506 (2002)
M. Hesse, J. Birn, M. Kuznetsova, Collisionless magnetic reconnection: Electron processes and transport modeling. J. Geophys. Res. **106**, 3721 (2001)
Y.M. Huang, A. Bhattacharjee, Scaling laws of resistive magnetohydrodynamic reconnection in the high-Lundquist-number, plasmoid-unstable regime. Phys. Plasmas **17**, 062104 (2010)
D. Innes, B. Inhester, W. Axford, K. Wilhelm, Bi-directional plasma jets produced by magnetic reconnection on the sun. Nature **386**, 811–813 (1997)
H. Isobe, K. Shibata, Reconnection in solar flares: Outstanding questions. Astron. Astrophys. **30**, 79–85 (2009)
H. Karimabadi, W. Daughton, J. Scudder, Multi-scale structure of the electron the electron diffusion region. Geophys. Res. Lett. **34**, 13104 (2007)
M. Karlicky, M. Barta, H. Meszarosova, P. Zlobec, Time scales of the slowly drifting pulsating structure observed during the April 12, 2001 flare. Astron. Astrophys. **432**, 705 (2005)
B. Kliem, M. Karlicky, A. Benz, Solar flare radio pulsations as a signature of dynamic magnetic reconnection. Astron. Astrophys. **360**, 715 (2000)
A. Klimas, M. Hesse, S. Zenitani, Particle-in-cell simulations of collisionless reconnection with open outflow boundaries. Phys. Plasmas **15**, 082102 (2008)
G. Lapenta, Self-feeding turbulent reconnection on macroscopic scales. Phys. Rev. Lett. **100**, 235001 (2008)
J. Lin, Y.K. Ko, L. Sui, J. Raymond, G. Stenborg, Y. Jiang, S. Zhao, S. Mancuso, Direct observations of the magnetic reconnection site of an eruption on 2003 November 18. Astrophys. J. **622**, 1251–1264 (2005)
Y. Litvinenko, S. Martin, Magnetic reconnection as the cause of a photospheric canceling feature and mass flows in a filament. Sol. Phys. **190**, 45–58 (1999)
N.F. Loureiro, A.A. Schekochihin, S.C. Cowley, Instability of current sheets and formation of plasmoid chains. Phys. Plasmas **14**(10), 100703 (2007)
Z. Ma, A. Bhattacharjee, Fast impulsive reconnection and current sheet intensification due to electron pressure gradients in semi-collisional plasmas. Geophys. Res. Lett. **23**, 1673 (1996)
F. Malara, P. Veltri, V. Carbone, Competition among nonlinear effects in tearing instability saturation. Phys. Fluids B **4**, 3070 (1992)
P. Martens, Yohkoh-SXT observations of reconnection. Adv. Space Res. **32**, 905–916 (2003)
S. Masuda, T. Kosugi, H. Hara, Y. Ogawara, A loop top hard X-ray source in a compact solar-flare as evidence for magnetic reconnection. Nature **371**, 495 (1994)
W. Matthaeus, S. Lamkin, Rapid reconnection caused by finite amplitude fluctuations. Phys. Fluids **28**, 303 (1985)
N. Narukage, K. Shibata, Statistical analysis of reconnection inflows in solar flares observed with SOHO EIT. Astrophys. J. **637**, 1122–1134 (2006)
L. Ni, K. Germaschewski, Y.M. Huang, B.P. Sullivan, H. Yang, A. Bhattacharjee, Linear plasmoid instability of thin current sheets with shear flow. Phys. Plasmas **17**, 052109 (2010)
E.N. Parker, Sweet's mechanism for merging magnetic fields in conducting fluids. J. Geophys. Res. **62**, 509 (1957)
H. Petschek, Magnetic field annihilation, in *AAS-NASA Symposium on the Physics of Solar Flares*, ed. by W. Hess (NASA, Washington, 1964), pp. 425–439. NASA SP-50
P. Pritchett, Geospace environmental modeling magnetic reconnection challenge: Simulations with a full particle electromagnetic code. J. Geophys. Res. **106**, 3783 (2001)

V. Roytershteyn, W. Daughton, L. Yin, B. Albright, K. Bowers, S. Dorfman, Y. Ren, H. Ji, M. Yamada, H. Karimabadi, Driven magnetic reconnection near the Dreicer limit. Phys. Plasmas **17**, 055706 (2010)
R. Samtaney, N.F. Loureiro, D.A. Uzdensky, A. Schekochihin, S.C. Cowley, Formation of plasmoid chains in magnetic reconnection. Phys. Rev. Lett. **103**, 105004 (2009)
M. Shay, J. Drake, B. Rogers, R. Denton, Alfvénic collisionless magnetic reconnection and the Hall term. J. Geophys. Res. **106**, 3759 (2001)
M. Shay, J. Drake, M. Swisdak, Two-scale structure of the electron dissipation region during collisionless magnetic reconnection. Phys. Rev. Lett. **99**, 155002 (2007)
L.S. Shepherd, P.A. Cassak, Comparison of secondary islands in collisional reconnection to hall reconnection. Phys. Rev. Lett. **105**, 015004 (2010)
K. Shibata, Evidence of magnetic reconnection in solar flares and a unified model of flares. Astrophys. Space Sci. **264**, 129–144 (1999)
K. Shibata, S. Tanuma, Plasmoid-induced-reconnection and fractal reconnection. Earth Planets Space **53**, 473 (2001)
K. Shibata, S. Masuda, M. Shimojo, H. Hara, T. Yokoyama, S. Tsuneta, T. Kosugi, Y. Ogawara, Hot-plasma ejections associated with compact-loop solar flares. Astrophys. J. Lett. **451**, 83–85 (1995)
K. Shibata, T. Nakamura, T. Matsumoto, K. Otsuji, T. Okamoto, N. Nishizuka, T. Kawate, H. Watanabe, S. Nagata, S. UeNo, R. Kitai, S. Nozawa, S. Tsuneta, Y. Suematsu, K. Ichimoto, T. Shimizu, Y. Katsukawa, T. Tarbell, T. Berger, B. Lites, R. Shine, A. Title, Chromospheric anemone jets as evidence of ubiquitous reconnection. Science **318**, 1591–1594 (2007)
A.N. Simakov, L. Chacón, Quantitative, comprehensive, analytical model for magnetic reconnection in hall magnetohydrodynamics. Phys. Rev. Lett. **101**, 105003 (2008)
T. Takizuka, H. Abe, A binary collision model for plasma simulation with a particle code. J. Comput. Phys. **25**, 205 (1977)
S. Tsuneta, H. Hara, T. Shimizu, L. Acton, K. Strong, H. Hudson, Y. Ogawara, Observation of a solar-flare at the limb with the Yohkoh soft-X-ray telescope. Publ. Astron. Soc. Jpn. **44**, 63–69 (1992)
M. Ugai, T. Tsuda, Magnetic field-line reconnection by localized enhancement of resistivity. J. Plasma Phys. **17**, 337 (1977)
D. Uzdensky, The fast collisionless reconnection condition and the self-organization of solar coronal heating. Astrophys. J. **671**, 2139 (2007)
D. Uzdensky, R. Kulsrud, Two-dimensional numerical simulations of the resistive layer. Phys. Plasmas **7**, 4018 (2000)
D.A. Uzdensky, N.F. Loureiro, A. Schekochihin, Fast magnetic reconnection in the plasmoid-dominated regime. Phys. Rev. Lett. **105**, 235002 (2010)
W. Wan, G. Lapenta, Electron self-reinforcing process of magnetic reconnection. Phys. Rev. Lett. **101**, 015001 (2008)
M. Yamada, Y. Ren, H. Ji, J. Breslau, S. Gerhardt, R. Kulsrud, A. Kuritsyn, Experimental study of two-fluid effects on magnetic reconnection in a laboratory plasma with variable collisionality. Phys. Plasmas **13**(5), 052119 (2006). doi:10.1063/1.2203950
M. Yan, L. Lee, E. Priest, Fast magnetic reconnection with small shock angles. J. Geophys. Res. **97**, 8277 (1992)
T. Yokoyama, K. Akita, T. Morimoto, K. Inoue, J. Newmark, Clear evidence of reconnection inflow of a solar flare. Astrophys. J. Lett. **546**, 69–72 (2001)